Pion-Nucleon Scattering in the Boundary-Condition Model. I. Inelastic Effects on S Waves*

H. GOLDBERG† AND E. L. LOMON

Department of Physics and Laboratory of Nuclear Science, Massachusetts Institute of Technology, Cambridge, Massachusetts

(Received 25 March 1963)

S-wave amplitudes for both $T=\frac{1}{2}$ and $T=\frac{3}{2}$ π-N scattering in the 0–500 MeV range are constructed by means of the boundary-condition model. Included in the Hermitian F matrix is a production channel in which the two outgoing pions are assumed strongly correlated in the $T=0$, $J=0^+$ state. The behavior of the amplitude so derived is in agreement with the present analyses of the experimental data, and shows in a simple manner the mechanism for obtaining a maximum in the cross section through the introduction of an inelastic channel.

I. INTRODUCTION

In the past few years several attempts have been made at an understanding of the $\pi-N$ interaction. In particular, dispersion relations for the $\pi-N$ partial wave amplitudes using the singularities derived from the Mandelstam representation, in conjunction with phenomenological representations of strong $\pi-\pi$ interactions in various channels, have been used by several authors[1,2] to explain the available s-wave amplitudes. The difficulties with these approaches have mostly involved rather severe approximations about the contributions to the dispersion integrals of the discontinuities across the $\pi+\pi\rightarrow N+\bar{N}$ cut (the circle cut) and the elastic cut in the complex s plane. It is the aim of this paper to outline an approach to the problem using the boundary-condition model (B.C.M.), which incorporates unitarity and as much of the analyticity as is desired, and which permits a direct comparison with the requirements of the relativistic theory.

In a recent paper[3] (hereafter referred to as FL) the application of the B.C.M. to the problems of elementary particle physics was discussed and justified on several grounds. The application to $\pi-N$ scattering was also mentioned. In Sec. II we shall repeat a few of the theoretical arguments in favor of the model with special reference to the $\pi-N$ case. In Sec. III the experimental s-wave data will be presented and discussed. Section IV will deal with the effects of inelastic channels as a possible explanation of some of the data. Section V will set forth both the single and multichannel forms of the B.C.M. and derive some of the pertinent equations. The $T=\frac{1}{2}$ and $T=\frac{3}{2}$ cases will be dealt with separately and the best fits will be presented in Sec. VI. Section VII will contain conclusions drawn from the fits and a discussion of further uses of the model for the $\pi-N$ interaction.

* This work is supported in part through funds provided by the Atomic Energy Commission under contract AT(30-1)-2098.

† IBM Predoctoral Fellow.

[1] J. Bowcock, N. Cottingham, and D. Lurie, Nuovo Cimento **19**, 142 (1961).

[2] J. Hamilton and W. S. Woolcock, Rev. Mod. Phys. (to be published). This contains references to earlier work by Hamilton and others.

[3] H. Feshbach and E. L. Lomon Ann. Phys. (N. Y.) (to be published).

II. RELEVANCE OF THE B.C.M. TO STRONG INTERACTIONS

The double spectral representation for the $\pi-N$ scattering amplitude contains terms of the form

$$\int ds' \int dt' \frac{\rho(s',t')}{(s'-s)(t'-t)}.$$

The limits of integration may be found by unitarity and the conservation laws. In particular, the double spectral function $\rho(s',t')$ for processes of the type in Figs. 1(a) and 1(b) vanish outside the shaded areas in Fig. 2.

At energies where inelastic scattering is not important, it may be hoped that we can represent the effects of the shaded strip α by a superposition of Yukawa potentials in deriving the asymptotic amplitude. However, if strip β [i.e., diagram 1(b)] plays an important part, then, as explained in FL, the interaction is extremely nonlocal and the boundary condition may dominate. (The form of the boundary condition will be given in Sec. V.) We shall try a pure B.C.M. in a first attempt, hoping that the potential tail contributions [Fig. 1(a)] will not cancel the important effects to be discussed. The supposition was made mostly for ease of computation, but it has turned

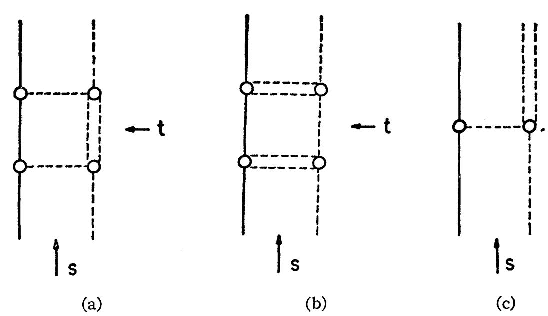

FIG. 1. (a) Lowest order contribution to α strip of double spectral function, giving rise to long-range "potential" effects. (b) Lowest order contribution to β strip of double spectral function, giving rise to shorter range B.C.M. effects. (c) Lowest order contribution to peripheral production. This may be related to the contribution of (a) through unitarity.

out to be sufficiently correct to accomplish the present objectives.

As shown in FL, the B.C.M. partial-wave amplitude is consistent with the analytic properties of the S matrix in the k^2 variable (where k is the momentum of the particles in their center of mass) as derived from the Mandelstam representation for the total amplitude, except possibly the asymptotic property. The various unphysical cuts are obtained by the choice of potential tail. For these reasons, we shall employ the model in this paper using full relativistic kinematics. The use of wave functions to derive the amplitude may be justified in that it gives a scattering amplitude with the correct analytic properties in the relativistic k^2 variable when the latter is formally substituted for the nonrelativistic one. Since we are not now concerned with the crossed $\pi+\pi \rightarrow N+\bar{N}$ reaction, the fact that crossing symmetry is not inherent in the model is not of importance in this case. Crossing between various partial wave channels (such as between the $T=\frac{1}{2}$, $J=\frac{1}{2}^-$ s-wave and the $T=\frac{1}{2}$, $J=\frac{1}{2}^+$ p-wave amplitudes) can later be imposed *ad hoc*, as has been done for the $\pi-\pi$ interaction in FL. This will place consistency requirements on the parameters involved. Inelastic unitarity, of great importance to the present discussion, is automatically contained in the model.

III. DISCUSSION OF THE s-WAVE DATA

A. $T=\frac{1}{2}$

We express the $T=\frac{1}{2}$ diagonal S-matrix element as $\eta_1 e^{2i\alpha_1}$, where η_1 and α_1 are real and $0\leqslant\eta_1\leqslant 1$. The available analysis of the data is plotted in Fig. 3.[4–8]

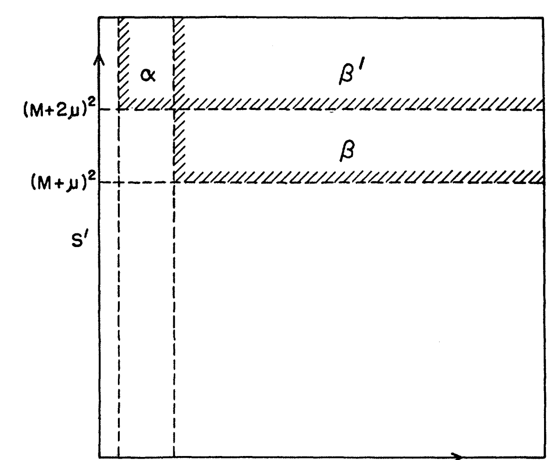

FIG. 2. Regions of the $s't'$ plane outside of which the double spectral function vanishes.

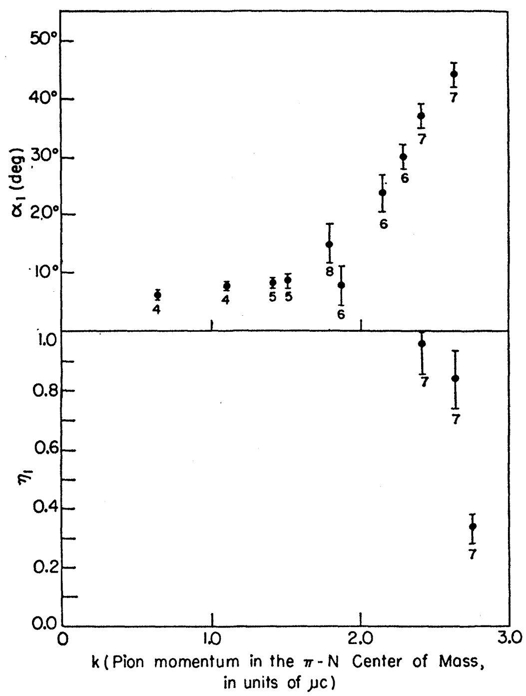

FIG. 3. $T=\frac{1}{2}$ s-wave elastic phase shift α_1 and inelastic parameter η_1 from analyses of experimental data. Reference to source of analysis is given by number at the point.

The outstanding feature in the energy behavior of the phase shift is the apparent "knee" not far above the inelastic threshold followed by a fairly sharp rise. This suggests a discontinuity of some kind and, thus, perhaps the onset of a new channel. The low-energy data have not been put into the plot but they are consistent with a scattering length $a_1=0.173\mu^{-1}$.[2] [Here we set $\hbar=c=1$, and μ is the charged pion mass. Lengths are thus measured in units of μ^{-1}, the pion Compton wavelength and momenta and energies in units μ. The scattering length a_1 is defined as $\lim_{k\rightarrow 0}(\alpha_1/k)$.] The data on η_1 show virtually no absorption until $k=2.4\mu$; then rather strong absorption seems to arise over a small energy interval, again suggesting the possible importance of the inelastic channel.

B. $T=\frac{3}{2}$

Here (see Fig. 4) we have no apparent structure effects in the phase shift a_3.[7–12] The absorption parameter η_3 has not been plotted since it is essentially 1 through-

[4] S. W. Barnes, B. Rose, G. Giacomelli, J. Ring, K. Miyake, and K. Kinsey, Phys. Rev. **117**, 226 (1960).
[5] H. Y. Chiu and E. L. Lomon, Ann. Phys. (N. Y.) **6**, 50 (1959).
[6] S. M. Korenchenko *et al.*, Dubna Report P-431, 1959 (unpublished).
[7] W. D. Walker, J. Davis, and W. D. Shepard, Phys. Rev. **118**, 1612 (1960).
[8] J. Deahl, M. Derrick, J. Fetkovich, T. Fields, and G. B. Yodh. Phys. Rev. **124**, 1987 (1961).
[9] G. E. Fisher and E. W. Jenkins, Phys. Rev. **116**, 749 (1959).
[10] *Proceedings of the 1958 Annual International Conference on High-Energy Physics, at CERN* (CERN, Geneva, 1958), p. 43, Fig. 7.
[11] B. Aubert *et al.*, CERN Report 61-11, 1961 (unpublished).
[12] E. H. Rogers, O. Chamberlain, J. H. Foote, H. M. Steiner, C. Wiegand, and T. Ypsilantis, Rev. Mod. Phys. **33**, 356 (1961).

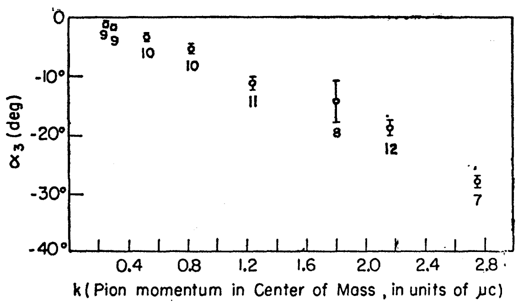

FIG. 4. $T=\frac{3}{2}$ s-wave elastic phase shift α_3 from analyses of experimental data. Inelastic parameter $\eta_3=1$. Reference to source of analysis is given by number at the point.

out the range of interest. The low-energy data are consistent with a scattering length a_3 lying between -0.090 and -0.110.[2,9] The absence of any appreciable absorption combined with the smoothness of α_3 as a function of k suggests that any inelastic channel controlling the $T=\frac{1}{2}$ behavior can have little, if any, effect in the $T=\frac{3}{2}$ channel. The slowness of the change of the slope of α_3 versus k from a constant negative value suggests the dominance of repulsive boundary condition type scattering which maximizes the negative rate of variation of the phase shift.[3]

IV. INELASTIC CHANNELS

The inelastic channel we shall consider in our attempt to explain the $T=\frac{1}{2}$ data is

$$\pi+N\rightarrow N+\pi+\pi.$$

In this way we recognize the possible importance of the α strip [see Figs. 2 and 1(a)] when we are above threshold. The model as presently used is unable to handle 3-particle channels, so that two of the three particles of the $N\pi\pi$ system must be assumed to be strongly correlated for our purposes.

Possible idealizations we may consider are

$$\pi+N\rightarrow\pi^*+N$$
$$\pi+N\rightarrow\pi+N^*.$$

For π^* one might be tempted to try the ρ meson ($T=1$, $J=1^-$). However, this would then appear in both the $T=\frac{1}{2}$ and $T=\frac{3}{2}$ states; also the threshold for such a reaction is too high for our domain of interest. Similarly, the N^* taken as the (3,3) isobar will appear in the $T=\frac{3}{2}$ state. One could eliminate both of these particles from the $T=\frac{3}{2}$ state, of course, by reducing the coupling to zero, but this seems too arbitrary a procedure.

One state in which there is mounting evidence that the two pions are strongly correlated, if not resonant, at a low energy in their center-of-mass system is the state of $T=0$, $J=0^+$. Such a two-pion system can be produced only in the $T=\frac{1}{2}$ channel and, hence, will not affect the $T=\frac{3}{2}$ elastic scattering. The justification for assuming a strong attraction or resonance at low energy for two pions in this state derives mainly from the experiments of Abashian, Booth, and Crowe,[13] Samios *et al.*,[14] and Richter.[15] In the first of these experiments the authors provided an explanation of their data in the $p+d\rightarrow He^3+2\pi$ (neutral) $p+d\rightarrow H^3+2\pi$ (charged) reactions by postulating a narrow $T=0$, $J=0^+$ resonance in the final state of the two pions. Truong[16] and Jacob, Mahoux, and Omnes[17] have suggested that the data could be explained by a nonresonant but strongly attractive interaction between the two pions in this state with a scattering length of the order of $1.5\mu^{-1}$. Results of Hamilton *et al.*[2] seem to support this hypothesis. Both these interpretations will be tested. The results of the model bear out the existence of a strongly attractive ($0,0^+$) state with a preference for the resonance interpretation. However, because of the crude approximation of the model used here and because of uncertainties in the data analysis, none of these possibilities is considered to be eliminated. Very recent data favors the scattering length fit, as mentioned in Sec. VII below.

V. THE BOUNDARY CONDITIONS

Conservation of flux at a radius r_0, when the particles may be described by configuration space wave functions outside $r=r_0$, is satisfied by the boundary conditions

$$r_0[dv(r)/dr]_{r=r_0}=fv(r_0) \tag{1}$$

in the one-channel case, and by

$$r_0\begin{bmatrix} du(r)/dr \\ dw(r)/dr \end{bmatrix}_{r=r_0}=\begin{bmatrix} f_1 & f_c \\ f_c & f_2 \end{bmatrix}\begin{bmatrix} u(r_0) \\ w(r_0) \end{bmatrix} \tag{2}$$

in the two-channel case. Here $v(r)$, $u(r)$, and $w(r)$ are the reduced radial wave functions in the various channels, whose values and derivatives are taken on the surface described by $|\mathbf{r}|^2=r_0^2$ in the relative coordinate $\mathbf{r}$. The channel described by $w(r)$ may have different kinetic energy and/or different orbital angular momentum from the channel described by $u(r)$. Similar equations, where $u(r)$ and $w(r)$ have had different orbital angular momenta but the same kinetic energy, have been previously used.[18] As used here, $u(r)$ and $w(r)$ will also have different kinetic energies associated with them.

The reality of f and the Hermiticity in general of the $\mathfrak{f}$ matrix is required by the unitarity of the system, while the reality of the $\mathfrak{f}$ matrix is a consequence of time-reversal invariance. (The matrix is related to F

[13] A. Abashian, N. E. Booth, and K. M. Crowe, Phys. Rev. Letters **5**, 258 (1960).
[14] N. P. Samios, A. N. Bachman, R. M. Lea, T. E. Kalogeropoulos, and W. D. Shepard, Phys. Rev. Letters **9**, 139 (1962).
[15] B. Richter, Phys. Rev. Letters **9**, 217 (1962).
[16] T. N. Truong, Phys. Rev. Letters **6**, 308 (1960).
[17] M. Jacob, G. Mahoux, and R. Omnès, Nuovo Cimento **23**, 838 (1962).
[18] H. Feshbach and E. L. Lomon, Phys. Rev. **102**, 891 (1956).

of FL by the relation $\mathfrak{f}=F+I$, where I is the unit matrix, due to our choosing to work with the reduced wave functions.)

Feshbach and Lomon[3] have shown that causality and considerations of the strength of the interactions involved will cause $\mathfrak{f}$ to be more or less energy-independent for r_0 at about the strong interaction distance characteristic of the β strip (in our case, at $\frac{1}{4}\mu^{-1}$). This energy independence is not, however, expected to hold for pole-type interactions such as the (3,3) $\pi-N$ channel, where there is no activity in the momentum transfer channel. (See Fig. 5.) A more general structure of $\mathfrak{f}$ to include these pole effects is discussed in FL.

VI. DETAILS OF THE MODEL AND THE FITTING OF THE DATA

A. $T=\frac{3}{2}$

Let us consider first the $T=\frac{3}{2}$ case. As there will be no absorption in this channel if the particle produced has $T=0$ (according to the hypothesis made in Sec. IV), the wave function $v(r)$ [see Eq. (1)] may be taken as $e^{-ikr}-e^{2i\alpha_3}e^{ikr}$, i.e., a scattered s wave, for $r>r_0$. α_3 is real. Application of the B.C. (boundary condition) of Eq. (1) implies

$$\beta \cot\alpha_3=\frac{f+\beta \tan\beta}{1-f(\tan\beta/\beta)}, \tag{3}$$

where $\beta=kr_0$.

In the scattering-length approximation, $k\cot\alpha_3=(1/a_3)$ for $k\to 0$. From Eq. (3) we get

$$f=r_0/(r_0+a_3). \tag{4}$$

To fix f, a_3 was varied slightly between -0.090 and -0.100, while r_0 was varied between 0.25 and 0.50. This left the one parameter, r_0, to fit the higher energy data, and this parameter was expected to stay within the above narrow limits required by its physical interpretation. An excellent fit to all data up to about 500 MeV (see Fig. 6) was obtained for $a_3=-0.098$ and $r_0=0.45$ (units of μ^{-1}). From Eq. (4), $f=1.28$. Since no potential tail was used, and a good fit was obtained, it is likely that diagrams of the kind 1(b) (representing the β-strip contributions) are largely responsible for the scattering. Note that r_0 is almost twice the estimate of $\frac{1}{4}\mu^{-1}$ obtained from consideration of Fig. 1(b). An explanation of this will be discussed in Sec. VII.

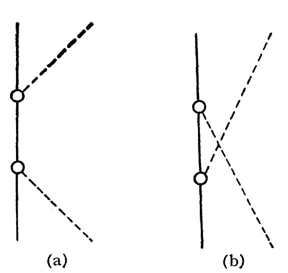

FIG. 5. Pole diagrams for π–N scattering.

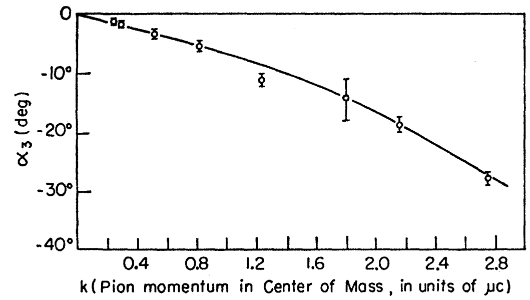

FIG. 6. α_3 obtained from single-channel B.C.M. Eq. (3). References to experimental points are given in Fig. 4.

B. $T=\frac{1}{2}$

General Formulation

Since there is inelasticity in this channel, the $\pi-N$ wave function $u(r)$ may be taken as $e^{-ikr}-\eta_1 e^{2i\alpha_1}e^{ikr}$ outside $r=r_0$, with η_1, α_1 real and $0\leqslant\eta_1\leqslant 1$. If a particle with definite mass m and $T=0$, $J=0^+$ is produced, $w(r)$ must be an outgoing p wave (by conservation of angular momentum and parity):

$$w(m,r)\propto(1+i/Kr)e^{iKr}.$$

K is the outgoing relative momentum and is given by

$$(K^2+m^2)^{1/2}+(K^2+M^2)^{1/2}=W, \tag{5a}$$

where $W=(k^2+\mu^2)^{1/2}+(k^2+M^2)^{1/2}$ is the total energy in the c.m. and the nucleon mass M is taken as 6.72μ.

For $W<M+m$ (i.e., below threshold for production of the mass m particle) we set $K=i\kappa$, and we have a decaying p wave given by

$$w(m,r)\propto(1+1/\kappa r)e^{-kr}.$$

κ is given by

$$(m^2-\kappa^2)^{1/2}+(M^2-\kappa^2)^{1/2}=W. \tag{5b}$$

This procedure is seen to be justified by asking that the B.C.M. S matrix have the proper analytic continuation in the complex k plane.[19]

Carrying through the calculations with the above wave functions, we get from Eq. (2)

$$r_0\left[\frac{du(r)}{dr}\right]_{r=r_0}=\left[f_1+\frac{f_c^2}{i[x-1/(x+i)]-f_2}\right]u(r_0), \tag{6}$$

where

$$x=Kr_0 \text{ for } W>M+m \text{ (above threshold)}$$
$$=i\kappa r_0 \text{ for } W<M+m \text{ (below threshold)}.$$

With this formulation and the definitions (5a) and (5b) the inelastic cut appears explicitly, and 2nd-order cusps (see Appendix) are obtained in $\alpha_1(k)$ at the momentum corresponding to the threshold for production of a particle with mass m [see Eq. (14)]. Such curves

[19] P. T. Matthews and A. Salam, Nuovo Cimento 13, 381 (1959).

are plotted in Figs. 8 and 10. As can be seen, the general nature of the curves is consistent with the data.

To take into account the width of the resonance, Eq. (6) is changed to

$$r_0\left[\frac{du(r)}{dr}\right]_{r=r_0}=\left[f_1+\int_{2\mu}^{\infty}\frac{\rho(m)dm}{i[x-1/(x+i)]-f_2}\right]u(r_0), \quad (7)$$

where x is a function of k^2 and m, and is given for each m by the definitions following Eq. (6) and Eqs. (5a) and (5b).

In this approximation, f_2 is independent not only of k^2, but also of m.

This integration procedure is equivalent to opening a continuous range of channels with varying m's, with a density $f_c^2(m)dm$ still independent of the external energy, viz., Eq. (2) becomes

$$\begin{aligned} r_0[du(r)/dr]_{r=r_0}&=f_1u(r_0)+\textstyle\sum_m f_c(m)w(m,r_0),\\ r_0[dw(m,r)/dr]_{r=r_0}&=f_c(m)u(r_0)+f_2w(m,r_0).\end{aligned} \quad (7a)$$

Then let $\sum_m f_c^2(m)\rightarrow\int\rho(m)dm$ in the resulting reduction.

Discussion of the ρ Function

If a stable particle with mass m^* is produced, we wish to have Eq. (7) reduce to the form of Eq. (6) with $m=m^*$. This can be done, clearly, by taking $\rho(m)=D\delta(m-m^*)$ with $D=f_c^2$. This suggests that, in general, we take $\rho(m)$ to be proportional to the $T=0$, $J=0^+$ $\pi-\pi$ cross section for elastic scattering at a total center-of-mass energy, m. The primary effects of the spread in the mass distribution will be accounted for by the equivalent spreading of the threshold effects in this choice of ρ. Thus, if we produce an unstable particle of average mass m^* and full width Γ at $\frac{1}{2}$ full intensity, $\rho(m)$ will be taken as a Breit-Wigner form of an s-wave resonance

$$\rho(m)=N_{\text{res}}\frac{D}{(m-m^*)^2+(\Gamma^2/4)[(m-2\mu)/(m^*-2\mu)]},$$

where

$$N_{\text{res}}=\frac{(\Gamma^2/2)[1-(\Gamma^2/16)(m^*-2\mu)^{-2}]^{1/2}}{(\pi/2)-\tan^{-1}\{[(-2(m^*-2\mu)+(\Gamma^2/4)(m^*-2\mu)^{-1}]\Gamma^{-1}[1-(\Gamma^2/16)(m^*-2\mu)^{-2}]^{-1/2}\}}. \quad (8)$$

The integration over m in Eq. (7) will then extend from $m=2\mu$ to $m=\infty$. The normalization factor N_{res} in Eq. (8) assures $\int_{2\mu}^{\infty} dm\rho(m)=D$. Thus, D should be the full equivalent of f_c^2 in the two-channel case.

On the other hand, suppose we have a nonresonant $\pi\pi$ system. In it the π's may still be correlated enough so that a boundary condition on the center-of-mass system is meaningful. In this case, we will let $\rho(m)$ take a form which is still proportional to the $(0,0^+)$ $\pi-\pi$ cross section $q^{-2}\sin^2\delta_0(q)$. Here $\delta_0(q)$ is the $T=0$, $J=0^+$ $\pi-\pi$ phase shift at pion momentum q in the $\pi-\pi$ center-of-mass system. In the scattering-length approximation

$$q\cot\delta_0(q)=a_0^{-1}, \quad (9)$$

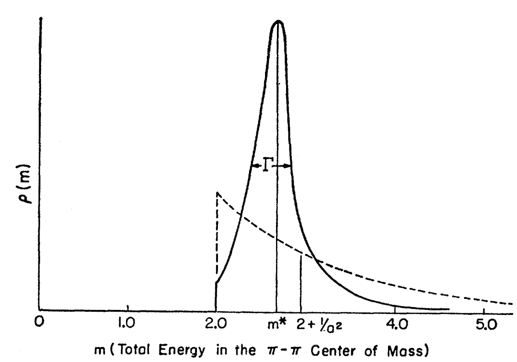

FIG. 7. The function $\rho(m)$ for the resonant (solid curve) and nonresonant (dashed curve) $\pi-\pi$ interactions.

from which we get

$$q^{-2}\sin^2\delta_0(q)=[a_0^{-2}+\mu(m-2\mu)]^{-1}, \quad (10)$$

since $m\approx 2\mu+q^2/\mu$ if the kinetic energy in the $\pi-\pi$ center-of-mass system is reasonably low. The same approximation was made in writing the resonant cross section. No major error is expected to result from this due to the integration to high m's since all quantities in the integrand fall off rapidly. Appropriately relativistic formulations of both the Breit-Wigner and scattering-length forms can and will be used when necessary. The main thing is that the Breit-Wigner form used has the correct behavior at $q\rightarrow 0$ $(m\rightarrow 2\mu)$ and around resonance $(m\approx m^*)$.

Thus, as an approximation in the nonresonant case we use Eq. (7) with

$$\rho(m)=N_{\text{scl}}\frac{D}{a_0^{-2}+\mu(m-2\mu)},$$

where

$$N_{\text{scl}}=\{\ln[a_0^2(m-2\mu)\mu+1]\}^{-1}. \quad (11)$$

The extension of this to the full effective range approximation is easy. This was done, but was not found to add results of further interest.

Curves of $\rho(m)$ versus m are shown in Fig. 7. The maximum in the Breit-Wigner curve is shown as occurring at $m=m^*$. This will be approximately so if $\Gamma\ll m^*$.

Derivation of the Elastic Phase Shift and Inelastic Parameter

In general, the equation from which η_1 and α_1 are derived is given by

$$r_0[du(r)/dr]_{r=r_0} = f_{\text{eff}}(k^2)u(r_0)\,, \tag{12}$$

where $f_{\text{eff}}(k^2)$ is generally a complex function of the variable k^2. $f_{\text{eff}}(k^2)$ is given by Eq. (6) in the stable particle production case, and by Eq. (7) (the expression in the square brackets) in the general case. We shall show that below threshold for the second channel $f_{\text{eff}}(k^2)$ is real, whereas above threshold it acquires a negative imaginary part which is directly related to the absorption. The threshold momentum for the production of a particle π^* is given by

$$k_0 = \frac{[(m_0-\mu)(m_0+\mu)(2M+m_0-\mu)(2M+m_0+\mu)]^{1/2}}{2(M+m_0)}\,, \tag{13}$$

where m_0 is the lowest mass of the π^*. In the pure particle case $m_0=m^*$. In the resonant and nonresonant two-pion cases $m_0=2\mu$.

Now we derive η_1 and α_1. Let

$$f_{\text{eff}} = f_{\text{eff}}(k^2)\,,$$
$$f_r = \operatorname{Re} f_{\text{eff}}(k^2)\,,$$
$$f_i = \operatorname{Im} f_{\text{eff}}(k^2)\,.$$

Writing $u(r)=e^{-ikr}-\eta_1 e^{2i\alpha_1}e^{ikr}$, and using Eq. (12), we obtain

$$\eta_1 e^{2i\alpha_1} = \frac{f_{\text{eff}}+i\beta}{f_{\text{eff}}-i\beta}e^{-2i\beta}\,, \tag{14}$$

where $\beta=kr_0$ as before. From this we obtain the following formulas for the desired quantities:

$$\eta_1 = \left[\frac{f_r^2+f_i^2+\beta^2+2\beta f_i}{f_r^2+f_i^2+\beta^2-2\beta f_i}\right]^{1/2}\,, \tag{15}$$

$$\beta\cot\alpha_1 = \frac{\beta\tan\beta+\bar{f}}{1-\bar{f}(\tan\beta/\beta)}\,, \tag{16}$$

where

$$\bar{f} = (1/2f_r)\{(f_r^2+f_i^2-\beta^2)+[(f_r^2+f_i^2+\beta^2)^2-4f_i^2\beta^2]^{1/2}\}\,.$$

Note that (16) is analogous to Eq. (3) in the one-channel case, except that now $\bar{f}$ has complicated energy dependence.

As stated, below threshold [$k<k_0$: see Eq. (13)] $f_i=0$. Thus, (15) reduces to

$$\eta_1 = 1\,,$$
$$\bar{f} = f_r = f_{\text{eff}}\,.$$

Now we explicitly exhibit the function $f_{\text{eff}}(k^2)$ using the integral formulation [Eq. (7)], keeping in mind that the stable-particle case may be obtained by letting $\rho(m)$ be a delta function at some mass m^*.

We define the following symbols:

$$y = r_0\kappa(k^2,m)\,,$$
$$z = r_0 K(k^2,m)\,,$$

where κ and K are given by Eqs. (5b) and (5a), respectively. With these definitions and Eq. (7) we obtain for

(i) $k<k_0$ (i.e., $W<M+2\mu$)

$$f_r = f_1 - \int_{2\mu}^{\infty} dm\,\rho(m)\frac{(y+1)}{y^2+(1+f_2)y+(1+f_2)}\,, \tag{17}$$
$$f_i = 0\,.$$

(ii) $k>k_0$ (i.e., $W>M+2\mu$)

$$f_r = f_1 - \int_{2\mu}^{W-M} dm\,\rho(m)\frac{f_2 z^2+(1+f_2)}{z^4-(1-f_2^2)z^2+(1+f_2)^2} - \int_{W-M}^{\infty} dm\,\rho(m)\frac{(y+1)}{y^2+(1+f_2)y+(1+f_2)}\,,$$

$$f_i = -\int_{2\mu}^{W-M} dm\,\rho(m)\frac{z^3}{z^4-(1-f_2^2)z^2+(1+f_2)^2}\,. \tag{18}$$

Unitarity requires that $0\leqslant\eta_1\leqslant 1$. From (15) we see that for this to be so we must have $f_i\leqslant 0$. This condition is seen to be satisfied in our model. From Eq. (18) we can see that f_i is never positive if $z^4-(1-f_2^2)z^2+(1+f_2)^2$ is never negative. Remembering that the $\mathfrak{f}$ matrix is real a sufficient condition is $|f_2|\geqslant 1$. Also sufficient is that the discriminant $(1-f_2^2)^2-4(1+f_2)^2\leqslant 0$. This is equivalent to $-1\leqslant f_2\leqslant 3$. Thus, it is also sufficient for $|f_2|\leqslant 1$. Thus, unitarity is fulfilled at all energies for any real $\mathfrak{f}$ matrix.

Note that in the pure particle case, m^* is necessarily less than $W-M$ for $k>k_0$, by the definition of k_0 in this case. Thus, the second integral in the expression for f_r in Eq. (18) vanishes due to ρ vanishing in the range of integration.

Fitting the Data

The slope of the phase shift at $k=0$ is given by the $T=\frac{1}{2}$ scattering length $a_1=0.173\mu^{-1}$.[2] The requirements that this slope be fitted by a pure B.C.M., i.e.,

$$r_0[du(r)/dr]_{r=r_0,k\to 0} = f_0[u(r_0)]_{k\to 0}$$

imposes the condition $f_0=r_0/(r_0+a_1)$ on the value f_0 of $f_{\text{eff}}(k^2)$ at $k^2=0$, where it is real. Thus, using Eq. (17) and the above condition, we obtain

$$\frac{r_0}{r_0+a_1} = f_1 - \int_{2\mu}^{\infty} dm\,\rho(m)\frac{y_0+1}{y_0^2+(1+f_2)y_0+(1+f_2)}\,, \tag{19}$$

where y_0 is $y(k^2,m)$ evaluated at $k^2=0$.

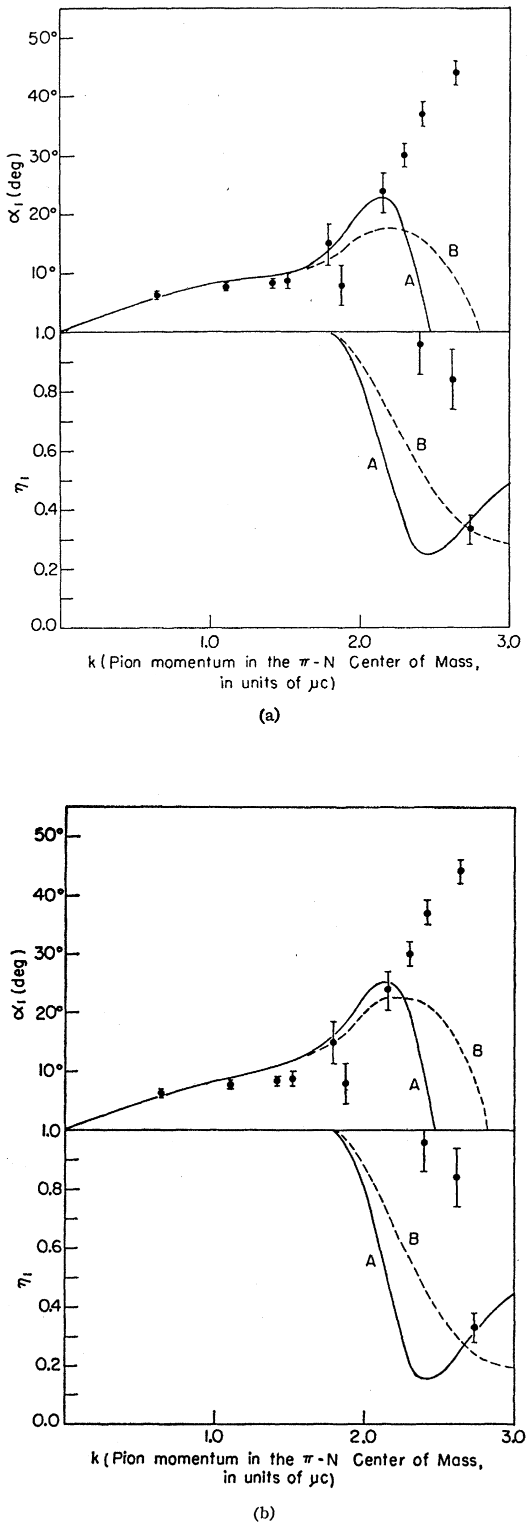

FIG. 8. (a),(b) α_1 and η_1 obtained from coupled-channel B.C.M. Eqs. (15) and (16). References to experimental points are given in Fig. 3. Parameters for various curves given in Table I. π–π interaction described by resonance at energy $m^*=2.30\mu$ (322 MeV), with $\Gamma=0$ ("ABC" resonance in stable-particle limit).

Thus, in the expression for f_r in Eqs. (17) and (18), we set $f_1=r_0/(r_0+a_1)+\Delta$, where Δ is the integral in Eq. (19) without the minus sign in front. In this way we determine one of the parameters, f_1, by fixing the scattering length.

Fixing a_1 at $0.173\mu^{-1}$, fitting r_0, f_2, and D (see "Discussion of the ρ Function" above) to higher energy data was done by trial and error on the IBM 7090 and 709 at MIT for the input $\pi-\pi$ interaction parameters given below. r_0 was varied in the range $(0.25$–$0.50)\mu^{-1}$, while extensive variation in f_2 and D was used. Cutoffs were used in all integrals having an infinite upper limit (for numerical purposes only, since everything is rapidly convergent), and the normalizations of the ρ functions were corrected to account for this. In the pure particle case, where $\rho(m)=D\delta(m-m^*)$, this integration procedure was, of course, unnecessary.

Several cases of the $T=0$, $J=0^+$ $\pi-\pi$ interaction were tried:

(i) Resonance at energy $m^*=2.30\mu$ (322 MeV) and zero width $(\Gamma=0)$. $\rho(m)$ is here taken as the delta function at the above m^*.

This is consistent with the results of Abashian, Booth, and Crowe[13] and Richter.[15] The width in these cases may have been up to 10 MeV (0.07μ) if the resonance interpretation is accepted, but the effect of this finite width was tested and found entirely negligible.

(ii) Resonance at average energy $m^*=2.83\mu$ (395 MeV) and width $\Gamma=0.36\mu$ (50 MeV). $\rho(m)$ in this case is given by Eq. (8).

These are the isotopic spin, energy, and average width deduced from the data of Samios *et al.*[14] from the two-pion mass plots. We try them with the $T=0$, $J=0^+$ assignment which seems most likely in a low-energy $\pi-\pi$ resonance that has been experimentally excluded from $T=2$.

(iii) Same as (ii), except zero width $(\Gamma=0)$.

(iv) Strong nonresonant interaction with $\pi-\pi$ scattering length $a_0=1.5\mu^{-1}$.

Formula (11) was used for $\rho(m)$.

This is an approximate value suggested by the conclusions in Refs. 2, 16, and 17.

(v) Same as (iv), except for $a_0=2.0\mu^{-1}$.

It was found that in all five cases an $r_0=0.45\mu^{-1}$ just as for $T=\frac{3}{2}$ was compatible with the best fits. This being so, f_1 was determined from Eq. (19) given D, f_2, and the ρ function. Thus, the fitting to higher energies, after having decided on this r_0, was done with the two remaining parameters D and f_2 for each of the five $\pi-\pi$ interactions assumed.

The presentation of the results for cases (i) to (v), in Figs. 8–12, respectively, is according to the following plan: The (a) and (b) parts of each figure each contain two sets of curves, labeled A and B, respectively. (Each set of curves contains a curve of α_1 and the corresponding η_1 curve.) The A sets in all the figures have

$f_2=-0.30$, the B sets $f_2=+0.40$ (chosen to illustrate the differences of behavior in these two areas of f_2).

In the (a) part of each figure, the parameter D was chosen for each of the A and B sets so that the α_1 curves have a behavior which is the same until about 180 MeV and which is in agreement with the experimental points plotted. After that the different characteristics of the A and B sets reflect the different ranges of parameters used.

In the (b) part of each figure, D was again chosen to give uniform behavior in α_1 until 180 MeV for the A and B sets, except that the curves lie somewhat higher than in the (a) part. This was done in order to attain greater proximity to the phase shifts at the higher energies.

Finally, the values of the parameters for each set of curves are given in Table I.

TABLE I. Parameters for curves in Figs. 8–12.

	$r_0=0.45\mu^{-1}$ Case	$a_1=0.173\mu^{-1}$ Fig.	Set	$f_0=r_0/(r_0+a_1)=0.72$ f_1	D	f_2
(i)	Resonance	8(a)	A	1.18	0.50	−0.30
	$m^*=2.30\mu$	8(a)	B	1.55	1.50	+0.40
	$\Gamma=0$	8(b)	A	1.27	0.60	−0.30
		8(b)	B	1.72	1.80	+0.40
(ii)	Resonance	9(a)	A	1.28	0.70	−0.30
	$m^*=2.83\mu$	9(a)	B	1.69	1.90	+0.40
	$\Gamma=0.36\mu$	9(b)	A	1.43	0.90	−0.30
		9(b)	B	1.94	2.40	+0.40
(iii)	Resonance	10(a)	A	1.35	0.80	−0.30
	$m^*=2.83\mu$	10(a)	B	1.73	2.00	+0.40
	$\Gamma=0$	10(b)	A	1.43	0.90	−0.30
		10(b)	B	1.94	2.40	+0.40
(iv)	Scattering	11(a)	A	1.29	0.80	−0.30
	length	11(a)	B	1.76	2.20	+0.40
	$a_0=1.50\mu^{-1}$	11(b)	A	1.44	1.00	−0.30
		11(b)	B	1.94	2.60	+0.40
(v)	Scattering	12(a)	A	1.24	0.65	−0.30
	length	12(a)	B	1.63	1.80	+0.40
	$a_0=2.00\mu^{-1}$	12(b)	A	1.36	0.80	−0.30
		12(b)	B	1.84	2.20	+0.40

VII. DISCUSSION OF RESULTS AND CONCLUSIONS

We have shown the applicability of the B.C.M. to one and two channel $\pi-N$ scattering, and have given a possible approximation for a mass distribution in the final channel. All cases attempted showed the correct qualitative trend, both in the elastic phase shifts α_1 and α_3 and in the inelasticity parameter η_1. Particularly to be stressed is the almost perfect fit to the $T=\frac{3}{2}$ data from 0–500 MeV through the use of the model with two parameters, coupled with the correct behavior in the more complex $T=\frac{1}{2}$ case. On the basis of the model, this strongly indicates that a $T=0$, $J=0^+$ low-energy $\pi-\pi$ resonance (or strong interaction) in the final state of a production channel is a controlling factor in $\pi-N$ s-wave scattering in the 200 to 400-MeV range.

Quantitatively, the use of the Samios resonance energy has given the best fit, while a nonresonant "scattering-length" fit is least adequate. A better fit is

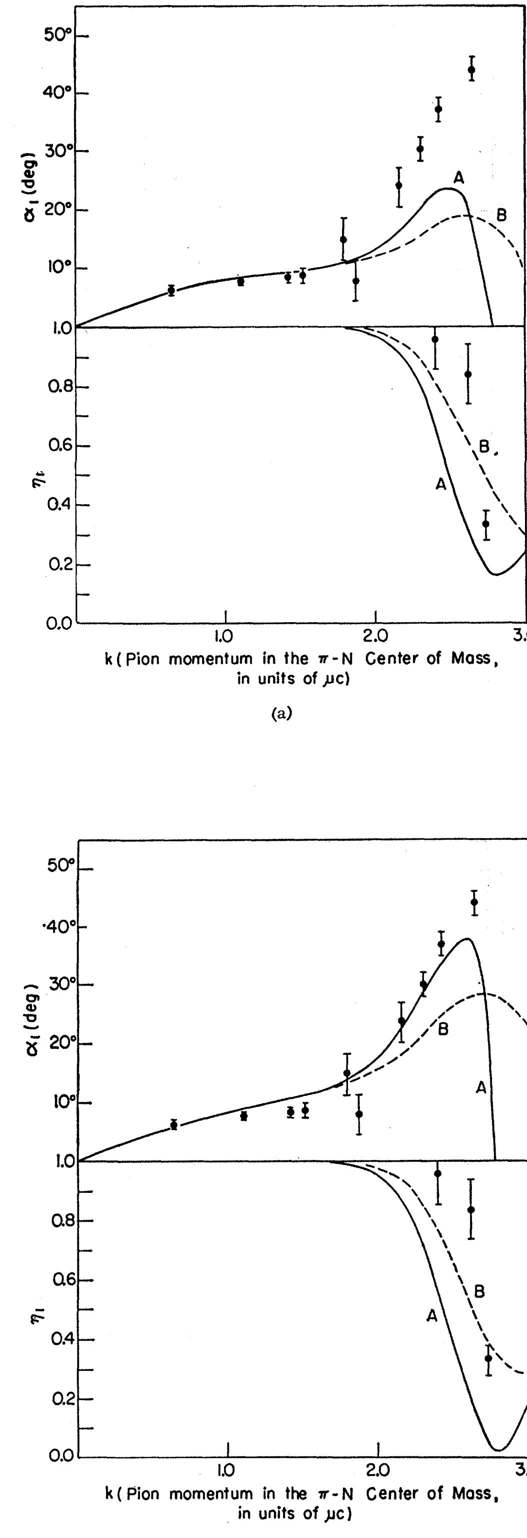

FIG. 9. (a),(b) Same as for Fig. 8 except here π–π interaction described by resonance at energy $m^*=2.83\mu$ (395 MeV), width $\Gamma=0.36\mu$ (50 MeV). ("Samios" resonance.)

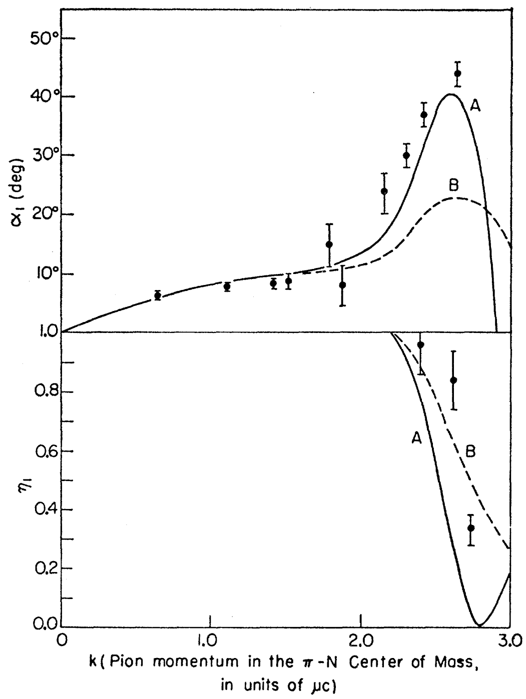

(a)

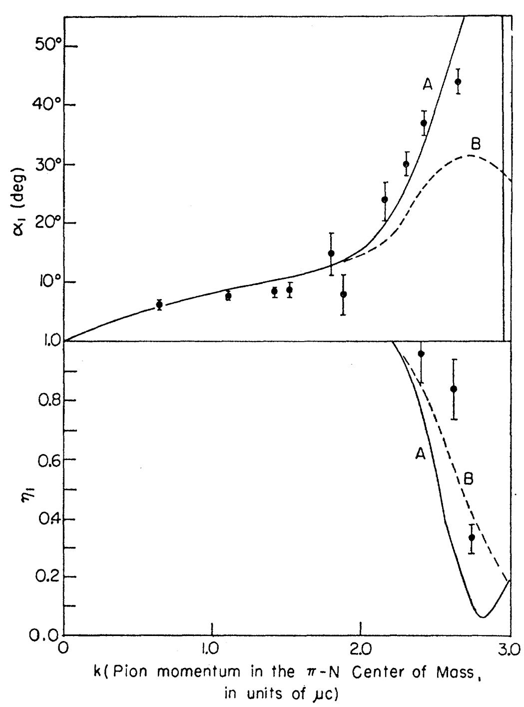

(b)

FIG. 10. (a),(b) Same as for Fig. 8 except here $\pi-\pi$ interaction described by resonance at energy $m^*=2.83\mu$ (395 MeV), width $\Gamma=0$. ("Samios" resonance in stable-particle limit.)

not necessarily to be expected due to the probable role of other inelastic processes at the highest energies considered.

These conclusions, of course, also depend on the accuracy of the data used and the uniqueness of its partial-wave-amplitude analysis. This production mechanism could be ruled out if future analyses showed, for instance, a value of η_1 very close to 1 in the range of interest, and a trend of α_1 toward negative values instead of a rise near threshold.

An amplitude analysis by Cence and Eandi,[20] of recent $\pi^{\pm}-p$ scattering experiments at energies in the range 500–1600 MeV by J. A. Helland *et al.*[21] and polarization data, has just been received. The α_1 and η_1 obtained in the analysis assuming a $D_{3/2}$ $\pi-N$ resonance in the $T=\frac{1}{2}$ state show excellent qualitative agreement with the behavior of these quantities as predicted from our model. Absorption in the $T=\frac{3}{2}$ s wave continues to be negligible, lending further support to the importance of the attractive $T=0$, $J=0^+$ 2π state in the s-wave scattering. Our scattering-length curves (Figs. 11 and 12, sets B) give the better agreement at these higher energies. The results of Walker *et al.*,[7] which favored the Samios resonance, were arrived at with much less experimental input. The Wigner condition on α_1 in the form $d\alpha_1/dk>-r_0$, whose possible violation is predicted by our model at energies above 400 MeV (notice the rapid drop of α_1 in Figs. 8–12) is also seen to be violated in this new experimental analysis near 600 MeV. As discussed below, this can be ascribed to the rapid onset of absorption which is not taken into account in Wigner's derivation.

Let us now discuss in more detail our results and their theoretical implications.

A. $T=\frac{3}{2}$

In this case we have apparently very well approximated the contributions of the β strip (Fig. 2) and have shown that even above threshold the effects of the α strip are negligible. However, the large value of $r_0(0.45\mu^{-1})$ compared to the value expected from the β strip $(0.25\mu^{-1})$ may be due to the long-range contributions of the α strip. These neglected contributions, in the absence of inelasticity, should be accounted for by the utilization of the unphysical cuts allowed in the model through the use of Hermitian potential tails in the construction of the wave functions to be used in the model. However, for the present, the data seem to be fitted well enough by substituting a somewhat enlarged core for the potential tail.

B. $T=\frac{1}{2}$

When a pure B.C.M. one-channel fit was attempted on low-energy data (0–120 MeV), we found that a

[20] R. Eandi, University of California thesis, UCRL Rept. No. 10629 (unpublished).

[21] J. A. Helland, T. J. Devlin, D. E. Hagge, M. J. Luongo, B. J. Moyer, and C. D. Wood, Phys. Rev. Letters **10**, 27 (1963).

radius r_0 of $0.35\mu^{-1}$ gave an excellent fit. With the subsequent introduction of the inelastic channel, however, a larger value of $0.45\mu^{-1}$ was necessary to keep the good fit below threshold and give a reasonable fit above. The reason for this may be seen by examining Fig. 1(c): The peripheral production of the "ABC" (or any pair of pions) takes place via an interaction whose range is longer than that of the interaction of Fig. 1(b), which contributes to pure B.C.M. scattering. As pointed out in the preceding paragraph and in FL, this long-range effect would best be taken care of by the use of a potential tail (in this case, a potential coupling of the two channels) in the derivation of the wave functions to be used in the construction of the scattering matrix from the B.C.M. This could be done numerically, but is avoided here for simplicity.

In the language of the Mandelstam relations, by introducing the inelastic channel we recognize the importance of the $T=0$ s-wave projection of the spectral function $\rho(s',t')$ in the α-strip approximation. To see this, we apply unitarity to Fig. 1(a) with the intermediate state of the two pions taken as $T=0$, $J=0^+$, and show that the desired projection of $\rho(s',t')$ is proportional to the cross section for the peripheral production of Fig. 1(c). This we then explicitly recognize as non-negligible.

It is also plausible that effects of the β' region (Fig. 2), which may have some importance for energies above threshold (due to the smallness of the energy denominator $s'-s$), can be approximated within the framework of the pure B.C.M.

Mechanism for a Maximum in the Elastic Cross Section

We now come to the most striking aspect of the results. According to the work of Ball and Frazer,[22] an amplitude with only the physical cut may give a sharp maximum in the cross section without the elastic phase shift necessarily going through 90°, if the inelasticity parameter drops fast enough to its unitary limit. They have suggested this as the mechanism for the higher $\pi-N$ resonances, with the ρ meson dominating the intermediate state in the α-strip approximation. However, there are very difficult problems with the imposition of unitarity both in their formulation and in subsequent more elaborate formulations.[23]

We now claim to have demonstrated clearly the effect discussed in Ref. 22, in the case of s-wave $\pi-N$ scattering. In addition, however, we have here the added advantage within the model of automatic unitarity. As seen from Figs. 8 and 10, the maximum is sharper the faster η_1 goes toward 0. The position of the maximum in the elastic phase shift is always above threshold. The rapid descent of α_1 with k after "resonance" does not violate the Wigner condition,[3] since

[22] J. S. Ball and W. R. Frazer, Phys. Rev. Letters **7**, 204 (1962).
[23] L. F. Cook, Jr. and B. W. Lee, Phys. Rev. **127**, 283 (1962).

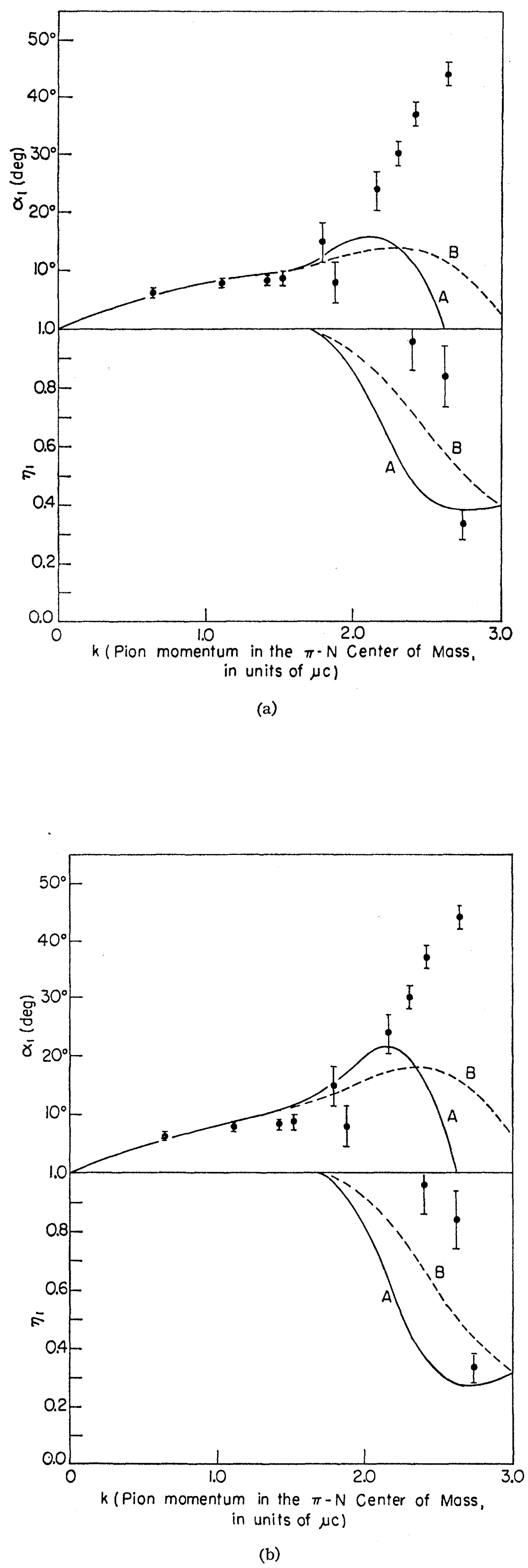

FIG. 11. (a),(b) Same as for Fig. 8 except here $\pi-\pi$ interaction described by scattering length of $1.5\mu^{-1}$.

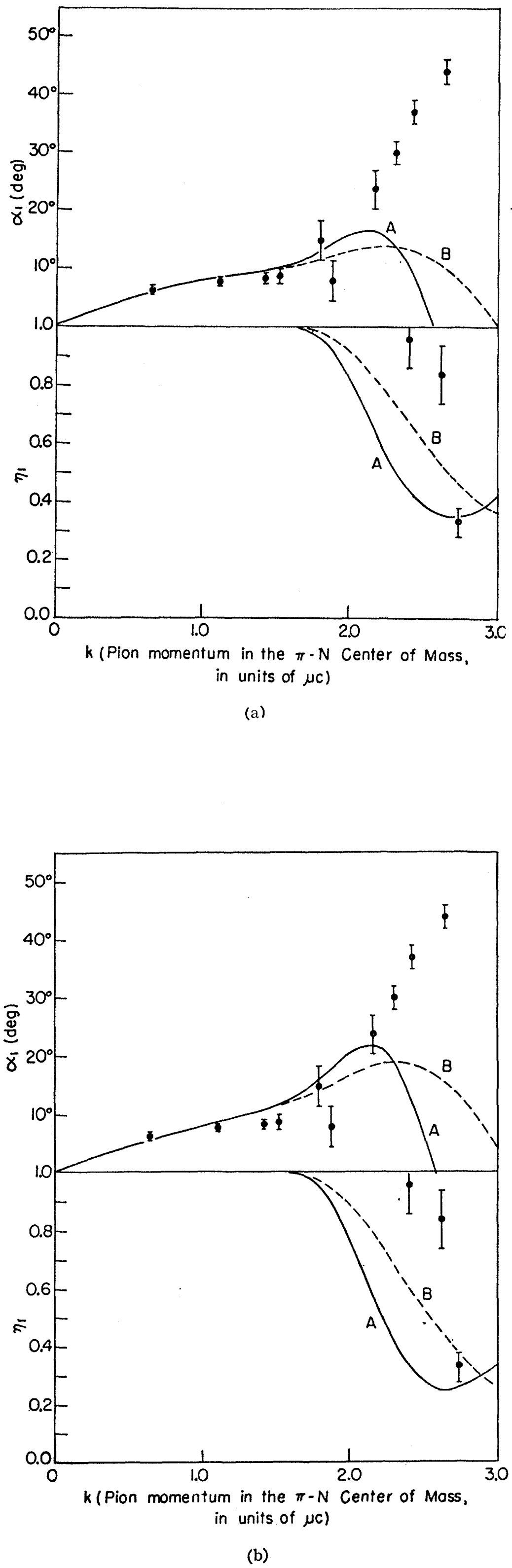

FIG. 12. (a),(b) Same as for Fig. 8 except here π–π interaction described by scattering length of $2.0\mu^{-1}$.

more than one channel is involved. The Wigner condition is taken care of by the constancy of the $\mathfrak{f}$ matrix as a function of k^2.

These questions will be explored more fully in work now in progress on the higher resonances. The aim will be to ascertain the role of the ρ (and/or the N^*) in an inelastic channel giving the size and shape of the cross section observed. The unitarity, desired analyticity, and reasonable underlying physical assumptions make the B.C.M. an attractive avenue of approach to these more complicated structures.

APPENDIX

Threshold Properties of Cross Sections and Phase Shifts

The general properties of cusps due to the opening of new channels are well known.[24–26] In this Appendix we obtain the detailed dependence for our interaction. The cusp behavior does not show up on our plots due to their small scale, but can be obtained from Eqs. (A15) and (A16) below.

We write the reduced radial wave function in channel 1 as

$$u(r)=\phi^*(r)+S\phi(r), \quad \text{for} \quad r>r_0, \tag{A1}$$

where $\phi(r)$ is an outgoing spherical wave of angular momentum l_1 (possibly in the range of a potential tail other than Coulomb), and normalized so that $\phi(r) \underset{r\to\infty}{\longrightarrow} (-i)^{l_1+1}e^{ikr}$. Then S is the usual diagonal matrix element $\eta e^{2i\alpha}$.

The wave function in channel 2 is $w(r)$, an outgoing spherical wave of angular momentum l_2.

Zero total flux at $r=r_0$ is obtained by requiring

$$\begin{aligned} r_0(du/dr)_{r=r_0}&=f_1u(r_0)+f_cw(r_0)\,,\\ r_0(dw/dr)_{r=r_0}&=f_cu(r_0)+f_2w(r_0)\,. \end{aligned} \tag{A2}$$

In the most general case, the $\mathfrak{f}$ matrix may have the energy dependence described in FL. We will assume this generality.

Since $w(r)$ is an outgoing wave asymptotically satisfying the free-particle equation, it can be written as

$$w(r)=\chi(Kr)e^{iKr}, \quad \lim_{r\to\infty}\chi(Kr)=\text{const},$$

where K is the outgoing momentum (pure imaginary below threshold). Therefore,

$$r_0(dw/dr)_{r=r_0}=\Theta w(r_0)\,, \tag{A3}$$

where $\Theta=Kr_0[(\chi'/\chi)+i]$ and the prime denotes differentiation with respect to Kr_0. Note that the form of Θ depends only on l_2.

[24] E. P. Wigner, Phys. Rev. **73**, 1002 (1948).
[25] G. Breit, Phys. Rev. **107**, 1612 (1957).
[26] R. G. Newton, Ann. Phys. (N. Y.) 4, 29 (1958).

Combining (A3), (A2), and using (A1) we get

$$S=-\frac{\Theta[f_1\phi^*-\beta\phi^{*\prime}]+[\beta f_2\phi^{*\prime}-(f_1f_2-f_c^2)\phi^*]}{\Theta[f_1\phi-\beta\phi']+[\beta f_2\phi'-(f_1f_2-f_c^2)\phi]}, \quad \text{(A4)}$$

where, as before, $\beta=kr_0$. Here the prime denotes differentiation with respect to β.

Remembering the Hermiticity of the $\mathfrak{f}$ matrix, this may be written as

$$S=-\frac{\Theta A^*+B^*}{\Theta A+B}, \quad \text{(A5)}$$

where A and B are complex functions of β and certain constants determined by the structure of the $\mathfrak{f}$ matrix. The important point is that, except for some accidental singularity at threshold in the structure of the $\mathfrak{f}$ matrix, A and B are continuous and have continuous derivatives in all orders at threshold. Hence, the character of discontinuity depends on Θ only and, hence, only on the angular momentum of the outgoing wave in the production channel.[25,26]

The elastic cross section

$$\sigma_{\mathrm{el}}=(\pi/k^2)|S-1|^2$$
$$=\left(\frac{4\pi}{k^2}\right)\frac{(\mathrm{Re}B)^2+(\mathrm{Re}A)^2[(\mathrm{Re}\Theta)^2+(\mathrm{Im}\Theta)^2]+(2\mathrm{Re}A\,\mathrm{Re}B)\mathrm{Re}\Theta}{|B|^2+|A|^2[(\mathrm{Re}\Theta)^2+(\mathrm{Im}\Theta)^2]+2\mathrm{Re}(AB^*)\mathrm{Re}\Theta-2\mathrm{Im}(AB^*)\mathrm{Im}\Theta}. \quad \text{(A6)}$$

Let us now choose r_0 large enough so that $w(r)$ satisfies the free-particle equation (approximately) for $r>r_0$. (We clearly cannot do this in the case of a Coulomb potential.) If $l_2=1$ (i.e., a p wave is produced), then

$$w(r)\propto[1+(i/Kr)]e^{iKr}=[1+(i/x)]e^{ix}, \quad \text{at} \quad r=r_0$$

using the definitions following Eq. (6) in the main article. From this and Eq. (A3),

$$\Theta(x)=(-1+ix^3)(1+x^2)^{-1}. \quad \text{(A7)}$$

Near threshold (on either side), x is small. Expanding and keeping terms to order x^3, we obtain

$$\Theta(x)\approx-1+x^2+ix^3+\cdots. \quad \text{(A8)}$$

Below threshold, we let $x\to iy$, $y=\kappa r_0$ [see Eq. (5b)]. Then near threshold,

$$\Theta(y)\approx-1-y^2+y^3+\cdots. \quad \text{(A9)}$$

Above threshold, we follow the main body of the article and formally substitute z for x. Then near threshold,

$$\Theta(z)\approx-1+z^2+iz^3+\cdots. \quad \text{(A10)}$$

$$\text{Let } E=W-M-\mu$$
$$=\text{incident kinetic energy}; \quad \text{(A11)}$$
$$E_{\mathrm{thr}}=m-\mu$$
$$=\text{threshold kinetic energy}.$$

From these definitions, and the assumption of small K, we obtain from Eqs. (5a) and (A11), that near threshold and below it

$$\kappa\approx\left(\frac{2mM}{M+m}\right)^{1/2}(E_{\mathrm{thr}}-E)^{1/2}. \quad \text{(A12)}$$

Above threshold

$$K\approx\left(\frac{2mM}{M+m}\right)^{1/2}(E-E_{\mathrm{thr}})^{1/2}.$$

Thus, below threshold, using (A9),

$$\Theta(E)\approx-1+\lambda^2(E-E_{\mathrm{thr}})+\lambda^3(E_{\mathrm{thr}}-E)^{3/2}+\cdots, \quad \text{(A13)}$$

where

$$\lambda=r_0\left(\frac{2mM}{M+m}\right)^{1/2}.$$

Above threshold, using (A10),

$$\Theta(E)\approx-1+\lambda^2(E-E_{\mathrm{thr}})+i\lambda^3(E-E_{\mathrm{thr}})^{3/2}+\cdots. \quad \text{(A14)}$$

From (A13) and (A14) we see that

(1) $\Theta(E)$ is continuous and has a continuous first derivative (with respect to the energy, E)at threshold.

(2) Approaching threshold from below,

$$d^2/dE^2(\mathrm{Re}\Theta)\to+\infty;$$
$$d^2/dE^2(\mathrm{Im}\Theta)=0.$$

Approaching threshold from above,

$$d^2/dE^2(\mathrm{Re}\Theta)=0;$$
$$d^2/dE^2(\mathrm{Im}\Theta)\to+\infty.$$

(3) At threshold, $\mathrm{Re}\Theta=-1$, $\mathrm{Im}\Theta=0$. Using these facts, and the fact that A and B are well behaved at threshold, we can say that, in this case

(1′) $\sigma_{\mathrm{el}}(E)$ is continuous and has a continuous first derivative (with respect to E) at threshold.

(2′) Approaching threshold from below

$$\frac{d^2\sigma_{\mathrm{el}}}{dE^2}\to\left(\frac{d\sigma_{\mathrm{el}}}{d(\mathrm{Re}\Theta)}\right)_{E=E_{\mathrm{thr}}}\left(\frac{d^2(\mathrm{Re}\Theta)}{dE^2}\right)_{E-E_{\mathrm{thr}}=0^-}$$
$$=\frac{6\pi\lambda^3}{k^2}\frac{\mathrm{Im}(AB^*)}{|B-A|^2}(\mathrm{Re}B-\mathrm{Re}A)^2(E_{\mathrm{thr}}-E)^{-1/2}. \quad \text{(A15)}$$

Approaching threshold from above,

$$\frac{d^2\sigma_{\mathrm{el}}}{dE^2} \to \left(\frac{d\sigma_{\mathrm{el}}}{d(\mathrm{Im}\Theta)}\right)_{E=E_{\mathrm{thr}}} \left(\frac{d^2(\mathrm{Im}\Theta)}{dE^2}\right)_{E-E_{\mathrm{thr}}=0^+}$$

$$= \frac{6\pi\lambda^3}{k^2}\,\frac{\mathrm{Im}(AB^*)}{|B-A|^2}(\mathrm{Im}A-\mathrm{Im}B) \times(\mathrm{Re}B-\mathrm{Re}A)(E-E_{\mathrm{thr}})^{-1/2}. \quad \text{(A16)}$$

Thus, the second derivative of the elastic cross section has an infinity at threshold when a p wave is produced.[25,26] The infinity may change sign if $(\mathrm{Re}B-\mathrm{Re}A)$ has a different sign from $(\mathrm{Im}A-\mathrm{Im}B)$. By looking at the curves in Fig. 8 or Fig. 10 we can see that this is what happened in our case. Of course, since the phase shift is a continuous function of the cross section, the same type of discontinuity will occur in a plot of α versus k as in σ versus E.

With an s wave in the outgoing channel, the usual type of cusp is found (first derivative infinite).[24] In general, if a channel with orbital angular momentum l is opened, the $(l+1)$st derivative will have a discontinuity at threshold, with no Coulomb forces present.[25,26]

It should be noticed that the above treatment is perfectly general, and can be applied to wave functions with any desired unphysical cut, insofar as an energy-dependent $\mathfrak{f}$ matrix, not singular at threshold, was permitted.

In some of our cases the produced particle is unstable. In these instances, "wooly" cusps[27] are obtained with properties which have been discussed in Ref. 27 The coupling scheme used in our formulation [Eq. (7a)] is consistent with that in the Nauenberg and Pais paper and, of course, is unitary.

[27] M. Nauenberg and A. Pais, Phys. Rev. **126**, 360 (1962).

PHYSICAL REVIEW VOLUME 131, NUMBER 3 1 AUGUST 1963

Modified K^* Exchange Model for ΛK^0 Production*

G. T. Hoff

The Enrico Fermi Institute for Nuclear Studies and Department of Physics, The University of Chicago, Chicago, Illinois

(Received 18 February 1963)

A model is proposed to explain simultaneously the backward peaking of the Λ particles in the reaction $\pi^-+p-\Lambda+K^0$, the large polarization observed, and the peak of the total cross section. The K^* exchange diagram and a resonant state in our channel are considered as the main contributions to the amplitudes. By assuming a resonant $p_{1/2}$ state, excellent fits to the angular distribution and polarization are obtained at a pion kinetic energy of 871 MeV and at an incident pion momentum of 1.01–1.05 BeV/c. A fairly good fit is obtained at a pion kinetic energy of 791 MeV. A new estimate for the $K^*\Lambda N$ coupling constant is given.

INTRODUCTION

IT is well known that the model of a K^* exchange proposed by Tiomno *et al.*[1] to explain the backward peaking of the Λ's produced in the reaction

$$\pi^-+p-\Lambda+K^0 \quad (1)$$

is incomplete, because it accounts neither for the observed large polarization of the Λ's nor for the peak in the total cross section at around an incident pion momentum of 1.03 BeV/c.

MacDowell *et al.*[2] have made fits to the angular distribution at pion kinetic energies of 960 and 1300 MeV by adding to the scheme a complex s wave. They obtained a satisfactory value for the average polarization only at the higher energy and needed two different products of coupling constants differing by a factor of 5 to obtain good fits to the angular distribution. Also, their work is incomplete in the sense that they did not attempt to fit the polarization dependence with angle.

In the present paper we propose a modification to the Tiomno scheme by adding a resonant partial wave. This model gives excellent fits to both the angular distribution and the polarization over a wide range of energy if we assume that the resonance is $p_{1/2}$. It gives also a fairly good fit to the energy dependence of the total cross section.

The idea of a $p_{1/2}$ resonance is not new. A $p_{1/2}$ or $p_{3/2}$ resonance was suggested by Kanazawa[3] in order to explain the peak in the total cross section. He ignored though the K^* exchange diagram, probably because at that time this particle was hypothetical, and considered instead the one-nucleon term and the Σ exchange term. In this paper we do exactly the opposite. We have a

* This work supported by the U. S. Atomic Energy Commission.

[1] J. Tiomno, A. L. L. Videira, and N. Zagury, Phys. Rev. Letters **6**, 120 (1961).

[2] S. W. MacDowell, A. L. L. Videira, and N. Zagury, Nucl. Phys. **31**, 636 (1962).

[3] Akira Kanazawa, Phys. Rev. **123**, 993 (1961).